Volumetric Imaging Using Fan-Beam Scanning with Reduced Redundancy 2D Arrays

Ira Wygant, Mustafa Karaman*, Ömer Oralkan, and Butrus T. Khuri-Yakub
E. L. Ginzton Laboratory
Stanford University, Stanford, CA 94304
Email: iwygant@stanford.edu
*Electronics Engineering Department, Işik University, Istanbul, Turkey
Email: karaman@isikun.edu.tr

***Abstract*— Phased array processing with a fully populated 2D array produces the best image quality but requires excessive number of active parallel front-end channels. Here we explore four array designs with reduced redundancy in spatial frequency contents. To minimize the number of firings we employ fan-beam processing, where 1D arrays are used to insonify 2D planar slices of the volume at successive firing events; echo signals are collected by the receive array elements. The array designs are compared based on simulated point spread functions, frame rate, motion susceptibility, and signal-to-noise ratio.**

I. Introduction

We have demonstrated a volumetric ultrasound imaging system based on a 5-MHz, 16×16-element capacitive micromachined ultrasonic transducer (CMUT) array [1]. In that system, the transducer array is flip-chip bonded to an integrated circuit (IC) that provides a pulser and preamplifier for each element of the array. To simplify the electronics for that system, only a single element can be active at a time for transmit and receive. We are now developing a multichannel version of the front-end IC [2]. We explored several array designs that were considered for implementation with the new IC [3]. This paper focuses on the four array designs described by Fig. 2 and Fig. 3 and proposes fan-beam scanning as a method to reduce the number of transmitted beams, thus increasing frame rate. The four fan-beam designs are compared with classic synthetic aperture (CSA) imaging and classic phased array (CPA) imaging. CSA imaging uses only a single element at a time and was used in our first implementation of the front-end IC. CPA imaging uses the full transmit and receive aperture; it provides the best image quality but demands the maximum number of transmit and receive channels. Comparisons are made based on a 16x16-element array. However, the results can be extended to larger arrays.

II. Reduced Redundancy Arrays and Fan-Beam Scanning

The coarray, the convolution of the transmit and receive apertures, illustrates how the apertures capture spatial frequency space (k-space). The lateral dimensions of the coarray correspond to k-space frequencies. The amplitude of the coarray at a particular k-space frequency shows the degree to which that frequency is redundantly captured. The coarray can be used as a design guide by looking for arrays that capture

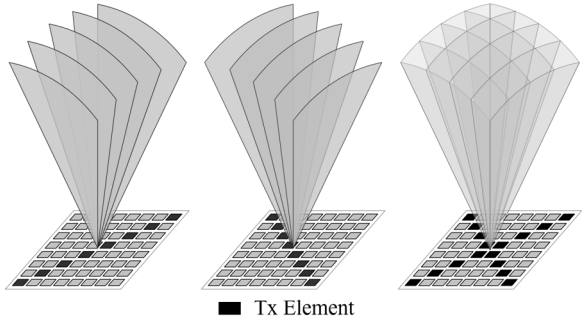

(a) For each arm of the X-shaped transmit aperture, $2N$ beams are transmitted across a 90° scan angle.

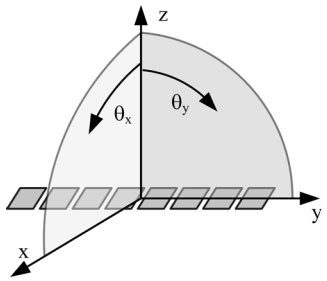

(b) Each arm of the X is treated as a 1D array.

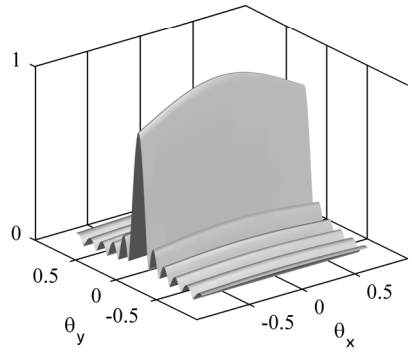

(c) The fan-beam created by the 1D array is broad in θ_x and can be steered in θ_y.

Fig. 1. Fan-beam scanning for an X-shaped transmit aperture and fully-populated receive aperture.

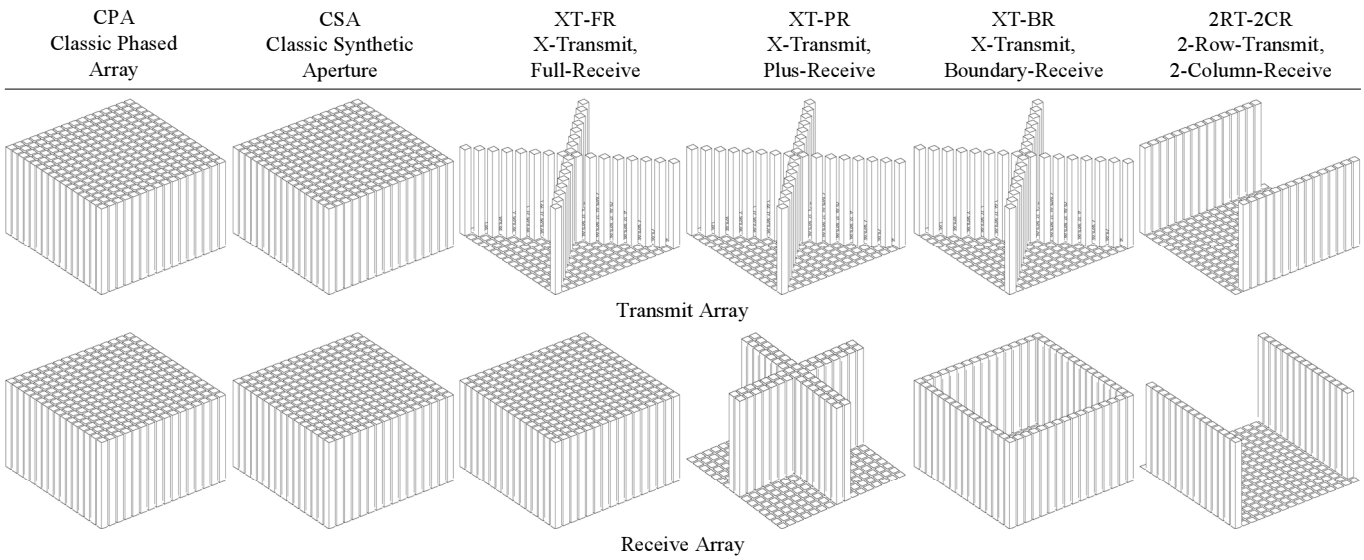

Fig. 2. Transmit and receive apertures.

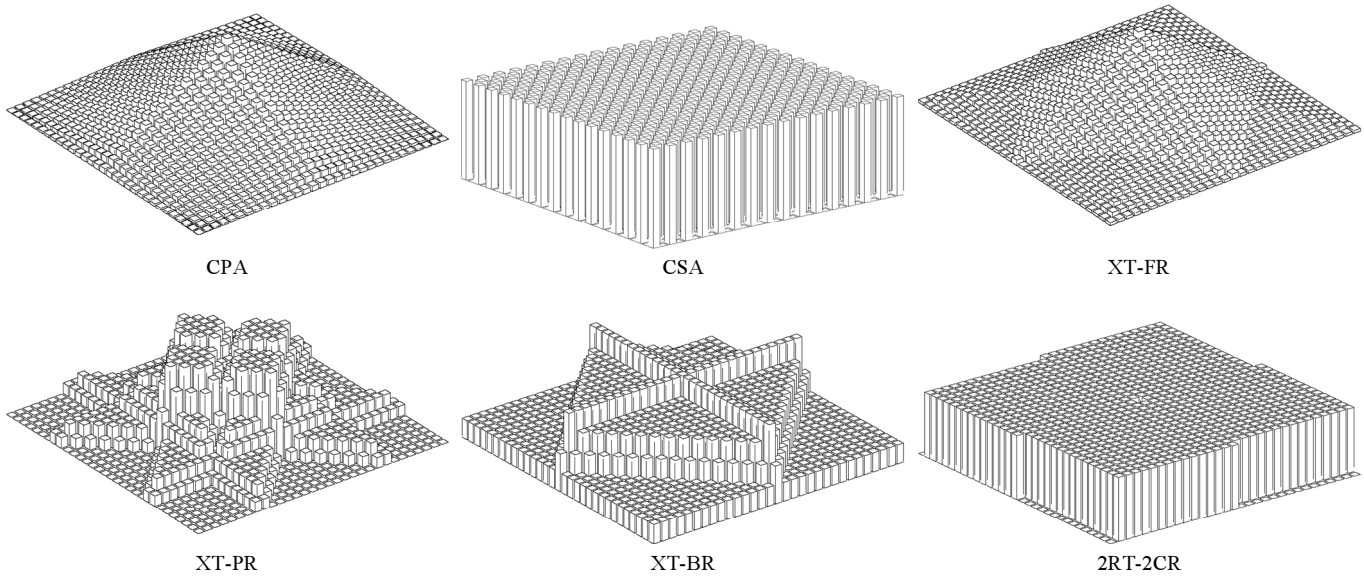

Fig. 3. Array design coarrays.

k-space with reduced redundancy. General array processing studies reported in the literature target to simplify the front-end by using a subset of active transmit and receive elements [4]–[11]. Here we present four two-dimensional array designs that have reduced redundancy in comparison with CPA imaging. For transmit apertures like a cross, which essentially consist of a small collection of 1D arrays in different orientations, we propose fan-beam scanning as a way to improve frame rate. To understand the advantages of fan-beam scanning, it is useful to compare the differences between two designs: full-transmit X-receive (FT-XR) and X-transmit full receive (XT-FR). FT-XR uses the full array for transmit and an X-shaped receive aperture. XT-FR (Fig. 2) uses an X-shaped transmit aperture and the full aperture for receive. Both designs have identical coarrays and thus identical point spread functions (PSFs). However, imaging with XT-FR can result in a substantially better frame rate. For a fully-populated transmit array with NxN elements, like that used for FT-XR, $\sqrt{2}N \times \sqrt{2}N$ transmit beams are needed for a 90° scan angle. In comparison, an X-shaped aperture requires only $4N$ beams since each arm of the X requires $2N$ transmit beams. The tradeoff made for increased frame rate is reduced SNR and increased motion susceptibility. Fig. 1 illustrates image acquisition using fan-beam scanning with XT-FR.

III. Simulations and Design Comparison

The on-axis and steered PSFs were simulated using the parameters shown in Table II. Two-dimensional cross-sections of the simulated PSFs are shown in Fig. 4. The cross-sections

TABLE I

COMPARISON OF ARRAY DESIGNS.

	Control		Fan-Beam Array Design			
	CPA	CSA	XT-FR	XT-PR	XT-BR	2RT-2CR
Tx Elements	16×16	16×16	2×16	2×16	2×16	2×15
Rx Elements	16×16	16×16	16×16	4×15	4×15	2×15
Active Tx elements	16×16	1	1×16	1×16	1×16	1×16
Active Rx Elements	16×16	1	16×16	4×15	4×15	2×15
Minimum Beams for 180° Scan Angle	32 × 32	-	45	45	45	45
Firings Per Frame	1,024	256	90	90	90	90
Maximum Frame Rate (3-cm Depth)	24	98	278	278	278	278
Image SNR (dB)	72	24	51	45	45	42
Motion Susceptibility Normalized to CPA	1	256	90	90	90	90

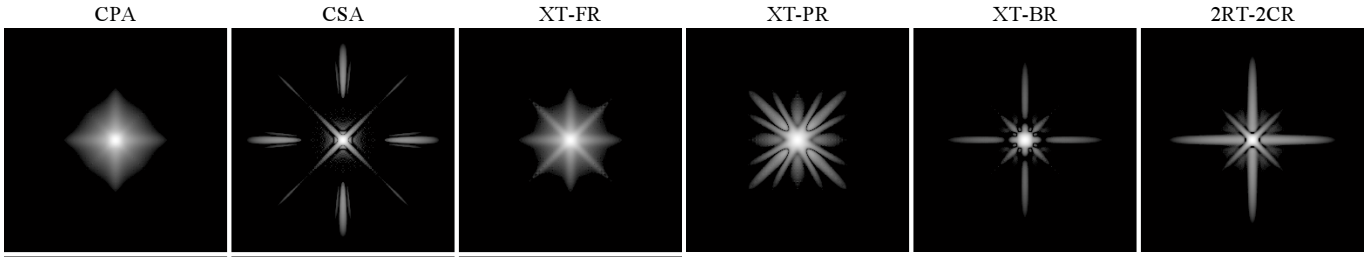

(a) $\phi\theta$–surface

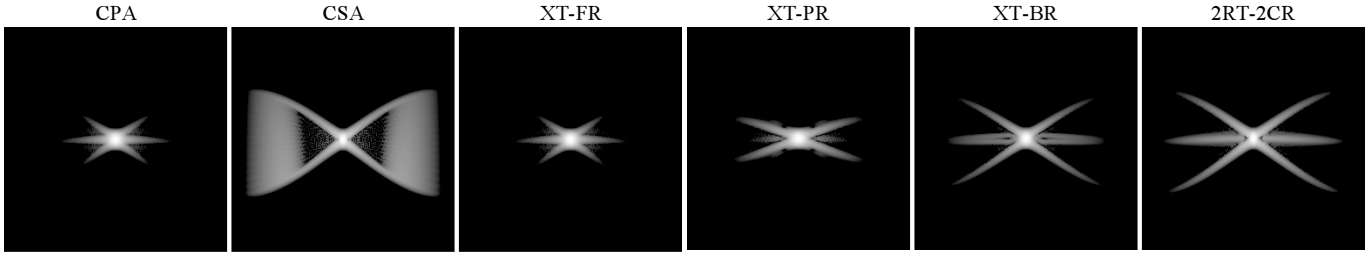

(b) $\rho\theta$–surface

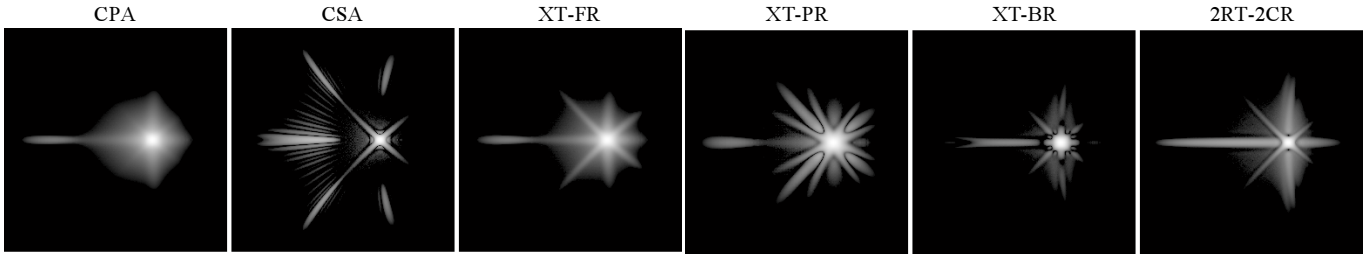

(c) $\phi\theta$–Surface, Steering Angle = 30°

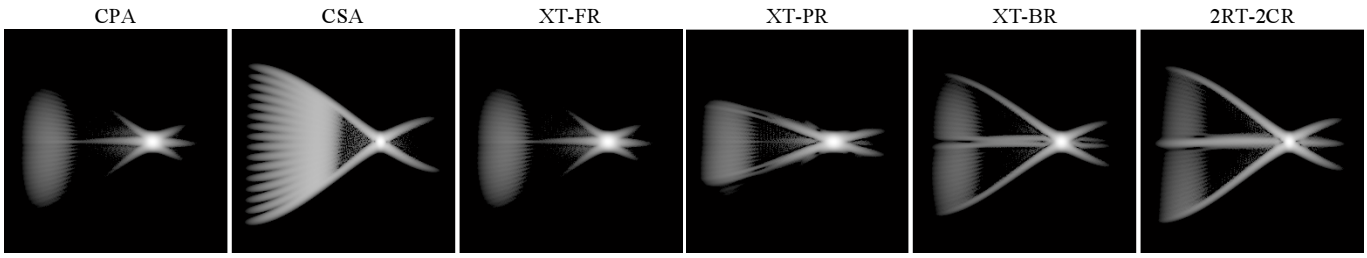

(d) $\rho\theta$–Surface, Steering Angle = 30°

Fig. 4. Simulated point spread functions shown with 50-dB dynamic range.

TABLE II

SIMULATION PARAMETERS

Elements in array	16×16
Element pitch	$0.5\lambda_0$
Frequency	5 MHz
Bandwidth	80% Gaussian pulse
Sampling frequency	250 MHz
Sound velocity	1540 m/s
Target distance	$f_{\#}$ of 4

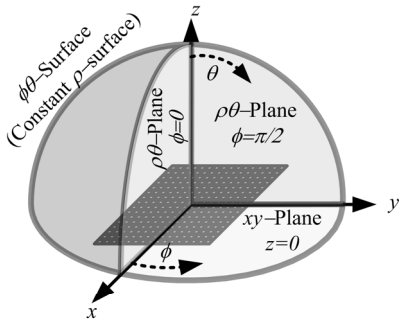

Fig. 5. Coordinate system for the point spread functions shown in Fig. 4.

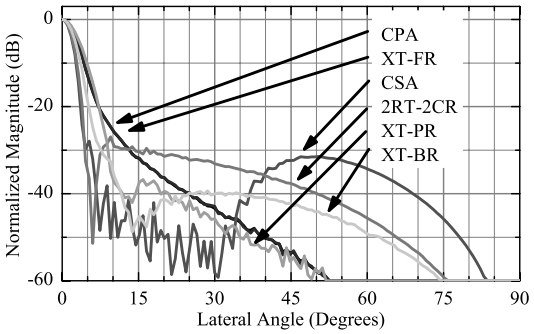

(a) Cross section of on-axis point spread function.

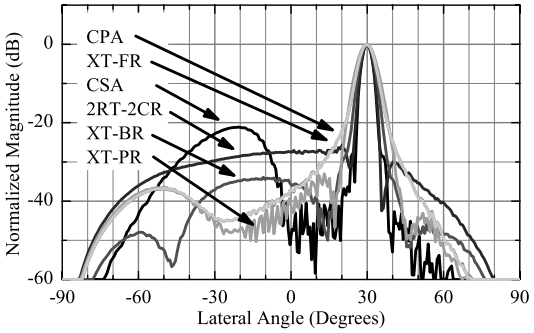

(b) Cross section of steered point spread function.

Fig. 6. Cross-sections of point spread functions integrated in ϕ.

are shown according to the coordinate-system shown in Fig. 5. One-dimensional lateral cross-sections of the PSFs are shown in Fig. 6.

Table I compares the frame rate, SNR, and motion susceptibility of the four designs. Frame rate is calculated based on the number of transmit beams and a 3-cm imaging depth (3-cm is desired for the targeted application of intracavital imaging). The SNR gain relative to a single A-scan is approximated as $N_t\sqrt{N_r}$ where N_t is the number of active transmit elements and N_r is the number of receive elements. Motion susceptibility is equal to the number of transmits required to generate the final pixel values for a beam. It is assumed that the number of receive channels equals the number of elements in the receive aperture. If a limited number of receive channels is assumed, then the frame rate and motion susceptibility would change accordingly.

IV. CONCLUSION

The four reduced-redundancy array designs evaluated here show significantly better performance than CSA imaging. XT-FR, XT-PR, and 2RT-2CR could all be implemented with minor modifications with our proposed design for a second-generation front-end IC. Thus, we expect that this new design will provide improved image quality in comparison with our first implementation. This improved image quality can be obtained while maintaining high frame rates by using fan-beam scanning to reduce the number of transmit beams.

ACKNOWLEDGMENT

Dr. Karaman is supported by TÜBİTAK of Turkey through grant 106M333.

REFERENCES

[1] I. O. Wygant et al., "An endoscopic imaging system based on a two-dimensional CMUT array: real-time imaging results," presented at the 2005 IEEE International Ultrasonics Symposium, Rotterdam, The Netherlands, Sep. 18–21, 2005.

[2] I. O. Wygant et al., "An integrated circuit with transmit beamforming and parallel receive channels for real-time three-dimensional ultrasound imaging," presented at the 2006 IEEE International Ultrasonics Symposium, Vancouver, Canada, Oct. 3–6, 2006.

[3] I. O. Wygant, M. Karaman, O. Oralkan, and B. T. Khuri-Yakub, "Beamforming and hardware design for a multichannel front-end integrated circuit for real-time 3D catheter-based ultrasonic imaging," presented at SPIE Medical Imaging 2006, San Diego, USA, Feb. 11–16, 2006.

[4] G. R. Lockwood and F. S. Foster, "Optimising the radiation pattern of sparse periodic two-dimensional arrays," *IEEE Trans. Ultrason., Ferroelect., Freq. Contr.,* vol. 43, pp. 15-19, Jan. 1996.

[5] J. A. Johnson, M. Karaman, B. T. Khuri-Yakub, "Coherent array imaging using phased subarrays-Part I: Basic principles," *IEEE Trans. Ultrason., Ferroelect., Freq. Contr.,* vol. 52, no. 1, pp. 37-50, Jan. 2005.

[6] J. A. Johnson, et al., "Coherent array imaging using phased subarrays-Part II: simulation and experimental results," *IEEE Trans. Ultrason., Ferroelect., Freq. Contr.,* vol. 52, no. 1, pp. 51-64, Jan. 2005.

[7] J. T. Yen, J. P. Steinberg, and S. W. Smith, "Sparse 2-D array design for real time rectilinear volumetric imaging," *IEEE Trans. Ultrason., Ferroelect., Freq. Contr.,* vol. 47, no.1, pp. 93-110, Jan. 2000.

[8] J. T. Yen and S. W. Smith, "Real-time rectilinear volumetric imaging," *IEEE Trans. Ultrason., Ferroelec., Freq. Contr.,* vol. 49 no. 1, pp. 114-124, 2002.

[9] A. Austeng and S. Holm, "Sparse 2-D arrays for 3-D phased array imaging-design methods," *IEEE Trans. Ultrason., Ferroelect., Freq. Contr.,* vol. 49, pp. 1073-1086, Aug. 2002.

[10] N. M. Daher, J. T. Yen, "Rectilinear 3-D ultrasound imaging using synthetic aperture techniques," in *Proc. IEEE Ultrason. Symp.,* pp. 1270-173, 2004.

[11] K.-S. Kim and T.-K. Song, "High volume rate 3-D ultrasound imaging using cross array based on synthetic transmit focusing," in *Proc. IEEE Ultrason. Symp.,* pp. 1409-1412, 2004.